Bol. Soc. Paran. Mat.
©SPM – E-ISSN-2175-1188
SPM: www.spm.uem.br/bspm

(3s.) **v. 2026 (44) 7** : 1–19.
ISSN-0037-8712
doi:10.5269/bspm.81400

Dynamics and Entropy Analysis for a Novel Sine-Cosine 5-D Hyper-Chaotic System and its Utilization for lightweight RGB Image Encryption

Hayder Kadhim Zghair, Adil Khudhair Bagheedh and Uday Jabbar Quaez*

ABSTRACT: In this paper, we presented a new sine-cosine 5-D hyper-chaotic system that has 2+ve and large maximum Lyapunov exponent compression with all system 5-D different previous studies with superior Kaplan-Yorke Dimension. This nonautonomous system consists of sixteen terms, nine of them non-linear, and every equation includes either a sine or cosine function with one zero unstable equilibrium point. We proved that the highly complex bounded attractor hyperchaotic system by information analysis, different analyses, including symmetric, SDIC, Kaplan-Yorke dimension, zero-one test, multistability, Lyapunov exponent, dissipative, equilibrium pt., stability proposed systems, bifurcation analysis, and Routh stability. Furthermore, we apply a 5-D sine-cosine hyperchaotic to generate a matrix (SSMK Generation) that has special properties. Moreover, we used the proposed system for RGB image encryption, which involves a two-part process. The initial part entails scrambling of colored images, while the second part employs a system in permutation, to give a better level of security while being easy to use to create a new algorithm based on the proposed system. It has proven the efficiency and speed of image encryption. We used MATLAB 2021b and Mathematica 13.2 to simulate and offer results.

Key Words: Lyapunov exponents, SSMK Generation, sine-cosine 5-D hyperchaotic system, Kaplan-Yorke dimension, SDIC, entropy.

Contents

* Corresponding author.
2020 *Mathematics Subject Classification:* 37D45, 94A17, 37M05.
Submitted January 17, 2026. Published April 11, 2026

1. Introduction

In the past decades, chaotic systems have been the subject of study for various fields in science and engineering [1,2,3] . The hyperchaotic system has two or more Lyapunov exponents which are type-positive [4,5] . That means its dynamics were expanded in many different directions so that hyperchaotic systems have more complicated dynamical behaviors than those of chaotic systems. Hyperchaos became the main topic in the research of nonlinear sciences due to its applications in several technological fields, including nonlinear circuits, lasers, encryption, neural networks, secure communications control, and synchronization. The dynamics of hyperchaotic systems have not been completely studied by mathematicians till now. Q. Yang et al introduced a 5-D hyperchaotic system which was obtained by the addition of a non-linear controller to a 4-D hyperchaotic which has $\mathfrak{L}_1 \succ \mathfrak{L}_2 \succ \mathfrak{L}_3 \succ 0$ where $\mathfrak{L}$ represent the Lyapunov exponent [6] . Y. Li et al proposed 5-D hyperchaotic and several image scramblers based on the proposed system [7]. R. Wang et al. constructed a new 5-D dynamical system; this system can show the hyperchaotic properties by using Multisim simulation and physical experiments, matched, and compared with each other, can show that the existence of phase chaotic portraits for this model as an attractor [8]. Vaidyanathan S. et al worked on a new 5-D hyperchaotic system having four wing hidden attractors. Researchers discuss the dynamical properties of this system [9]. Zaid J. Kubba et al designed a lightweight cryptographic system by applying a novel 5-D chaotic system. D. Fang et al designed a PRN sequence by using a 5-D hyperchaotic system, which produces a more complicated dynamical characteristic than low-low-dimensional systems [10]. Tao Wang et al. proposed a new 5-D 3-leaf chaotic attractor and used it in image encryption applications [11]. Xu Chang Biao et al. proposed a new 5-D hyperchaotic system. This system may have several types of equilibrium states by changing its parameters to form a stable hyperbolic type, and a non-hyperbolic unstable type [12]. Lei Ya et al. introduced a 5-D multistable hyperchaotic system. The system has various types of coexisting attractors, hyperchaotic, chaos, limit cycles, and periods [13]. M. Kaur et al introduced a novel multistable hyperchaotic system and discussed its applications in image scrambler [14]. SJ Sheela et al worked on an image scrambler algorithm that depends on a 5-D hyperchaotic system to have a high level of security. The chaotic sequences that have been generated from this system are used for the permutation of the plain image with a Sudoku matrix to generate a scrambler image [15]. In 2022 A. A.-H. Al-Shamery et al improved AES using a novel hyperchaotic system that will be suitable for image scrambling [17,16], .We donated SDIC to sensitive depending on the initial condition,secret scrambling matrix Key (SSMK) represents a secure storage matrix key and denoted r the correlation coefficient. Table 5. Comparing the analysis sine - cosine 5-D hyperchaotic with the different 5-D in the previous paper. The aim and objective of this research paper have been condensed into the following statements.:

1. Introduction to the new Sine-Cosine two-wing 5-D system and analysis of its which proved hyperchaotic dynamical behavior, to confirm the boundedness of the system based on analytic and numerical methods.

2. To employ entropy analysis of the proposed system in order to identify chaotic regions and to characterize its dynamical behavior.

3. It has a maximum Lyapunov exponent. $\mathfrak{L}_1 = \mathbf{15.0210}$ and superior Kaplan-Yorke dimension, which means this system shows high-complexity behavior, also, calculated Routh stability [18], and additional equilibrium pt. , and study stability for the sine-cosine 5-D system, to prefer a bifurcation analysis to determine parameter ranges that induce transition from stable state to chaotic behavior via periodic behavior.

4. A new Algorithm to generate $matrix_{\ 128\times128}$ (SSMK Generation) have special properties of which this matrix is symmetric, and every number between 0 to 255 are evenly distributed throughout each column and row without repeating.

5. A new algorithm for the RGB image scrambler algorithm based on the proposed system.

6. A comprehensive security analysis of the proposed scheme with another system.

The remainder of this paper is organized as follows. Section 2 introduces the Sine-Cosine Hyper-chaotic 5-D System. Section 3 presents the Entropy Analysis of the system. In Section 4, we propose an RGB Image Encryption Scheme based on the hyper-chaotic system. Section 5 discusses the Analysis of Security Factors and provides Computational Results. Section 6 presents the Results and Decision, while Section 7 concludes the paper by summarizing the key findings and insights.

2. Sine-Cosine Hyperchaotic 5-D System

2.1. System Description

In this subsection, we present a nonautonomous system consisting of sixteen terms containing nine nonlinear terms $y\ x$,$x\ z, y\ z$, and $w\ z$ quadratic cross-product also every equation contains either sine or cosine. a novel 5-D Sine-cosine two-wing hyperchaotic system as described as follows:

$$\left.\begin{array}{c} \dot{x} = -\alpha\ x + \beta\ y - ucosw \\ \dot{y} = -\eta\ y + \sigma\ x - \mho\ \ x\ z + x\ sinu \\ \dot{z} = \ -\ \xi\ z\ +\ x +\ \varrho\ w\ sinx \\ \dot{u} = -\psi\ u + \delta\ w\ z -\ ysinz \\ \dot{w} = -\tau w - y\ z - \eta\ x \sin y \end{array}\right\} \tag{2.1}$$

The state of the proposed system belonged to R^5 represent by $(x, y, v, w, z)^T$ Where 0.001-time step size for solving (2.1) and the ten parameters positive of the proposed system are represented by $(\alpha, \beta,\ \eta, \sigma,\ \mho,\ \xi, \varrho, \psi, \delta, \tau)$. Where $\alpha = 10.2$, $\beta = 12$, $\eta = 5.1$,$\sigma = 30$,$\mho = 2.5$, $\xi = 6$, $\varrho = 3$, $\psi = 1.1$, $\delta = 4$ and $\tau = 1$, and $x(0) = 0.5$, $y(0) = 2$, $z(0) = 1.5$, $v(0) = 6$, $w(0) = 1$, where β and ψ are control parameters in Fig.1 . The behavior of the proposed system shows phase chaotic portraits for this system. Fig(1-a). show two-wing phase chaotic portraits of two dimensions in x-y, Fig. (1-b). Show two-wing phase chaotic portraits of two dimensions in x-z, Fig. (1-c). Show phase chaotic portraits of three dimensions in x-y-z, and Fig. (1-d). Show phase chaotic portraits of three dimensions in x-z-w.

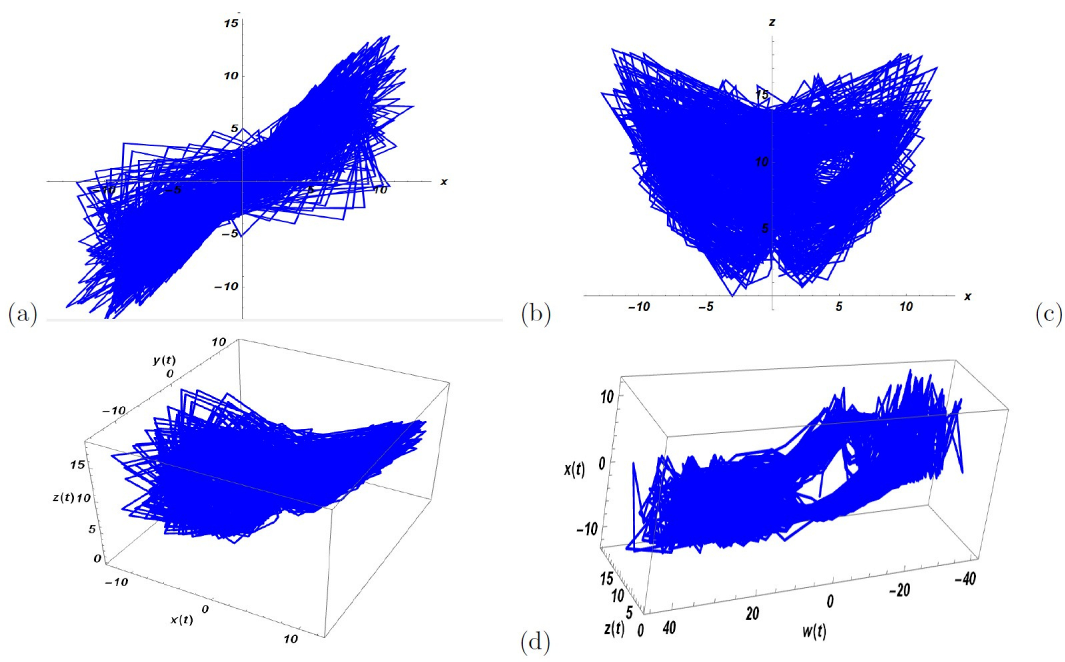

Figure 1: Shows phase chaotic portraits of a new sine-cosine hyperchaotic 5-D system.

2.2. Chaotic Dynamics

Symmetric, SDIC, Kaplan-Yorke Dimension, $\mathfrak{L}$, and Zero-One Test

.

Symmetric: A new sine-cosine hyper-chaotic 5-D system is invariant and therefore system 2.1 w.r.t z-axis is symmetric. Under the coordinated transformation: (w, v, z, x, y) =(-w, - v, z, -x, -y).
The Lyapunov exponent ($\mathfrak{L}$)Wolf A.[14]: using Jacobin Matrix when $\alpha = 10.2$, $\beta = 12$, $\eta = 5.1$, $\sigma = 30$, $\mho = 2.5$, $\xi = 6$, $\rho = 3$, $\psi = 1.1$, $\delta = 4$ *and* $\tau = 1$. are calculated by MATLAB after 10000 iterations, and 0.001 represents the step size, found that this system has
$\mathfrak{L}_1 = \mathbf{15.0210}$, $\mathfrak{L}_2 = \mathbf{0.78262}$, $\mathfrak{L}_3 = -\mathbf{0.62597}$, $\mathfrak{L}_4 = -\mathbf{10.5034}$and $\mathfrak{L}_5 = -\mathbf{31.0467}$
Therefore, the proposed system 2.1 is chaotic because $\mathfrak{L}_1 \succ 0$. In addition, system 2.1 is hyperchaotic because $\mathfrak{L}_1 and\ \mathfrak{L}_2 \succ 0$. Fig 2.1. shows the five Lyapunov exponents for the system 2.1, where $\mathfrak{L}_1,\ \mathfrak{L}_2 \succ 0$, $\mathfrak{L}_3 \simeq 0$, $\mathfrak{L}_4 and\ \mathfrak{L}_5 \prec 0$.
Kaplan-Yorke dimension ($\wp_{KY}$) [4] since $\sum_{i=1}^{4} \mathfrak{L}_i \succ 0$ and $\sum_{i=1}^{5} \mathfrak{L}_i \prec 0$ then $\wp_{KY} = 4 + \frac{\sum_{i=1}^{4} \mathfrak{L}_i}{|\mathfrak{L}_5|} = 4.8675$, after order $\mathfrak{L}_1 \succ \mathfrak{L}_2 \succ \mathfrak{L}_3 \succ \mathfrak{L}_4 \succ \mathfrak{L}_5$,Due to its fractal nature, the 5-D Sine-cosine two-wing hyperchaotic system produced non-periodic orbits as a result of the fractional Lyapunov dimension.

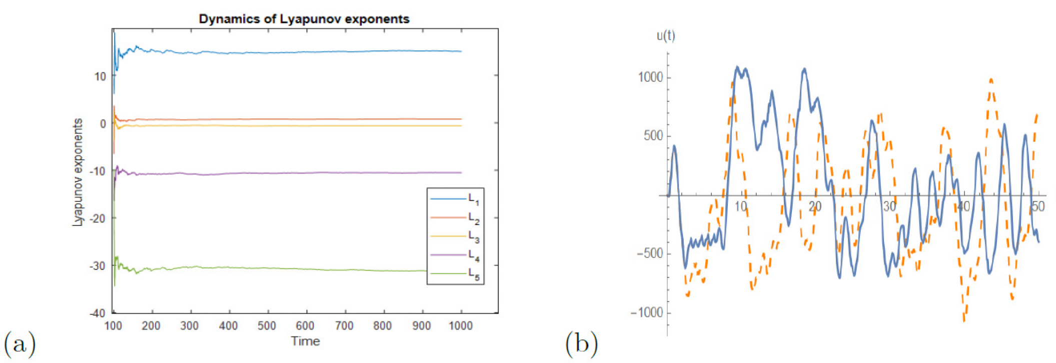

Figure 2: dynamics for system 2.1 (a) Lyapunov exponent (b) SDIC w.r.t w(t) when the tiny change in $\boldsymbol{w(0) = 1 + 10^{-14}}$.

The proposed system 2.1 is sensitive to any change in parameters or initial conditions. Fig.(2-b) shows a tiny change in initial condition w (0) for the dashed line results in a divergent path compared to system 2.1 solid line while the other initial condition remain unchanged. Furthermore, the system is multistability, which means there exist two solutions with various initial conditions, Fig. 3. proves the multistability of a new sine-cosine 5-D hyper-chaotic with two initial conditions.

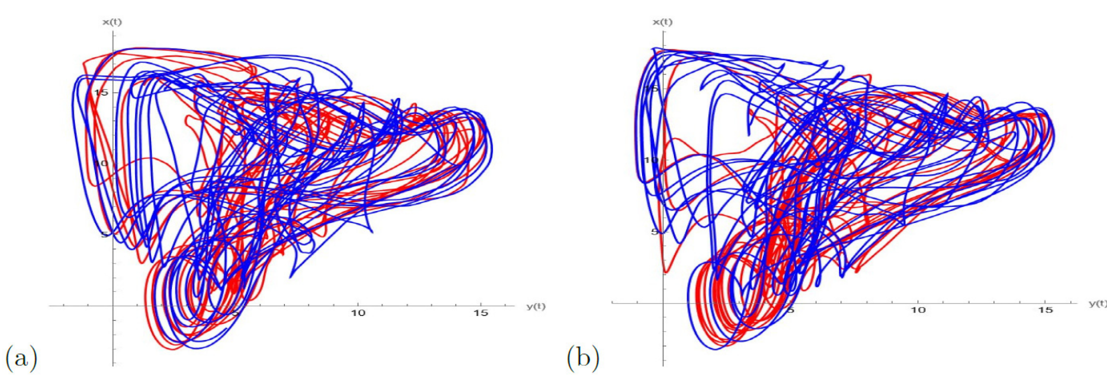

Figure 3: proves the multistability of a new sine-cosine 5-D hyper-chaotic system.a) Blue (4,4,4,4,4) and Red (3,3,3,3,3) , b) Blue (6,6,6,6,6) and Red (1.5,1.5,1.5,1.5,1.5)

Zero-one Test [20,19] is one of the most common methods to test chaotic systems that separate chaotic from nonchaotic dynamical systems by the values $\mathcal{K}$ when $\mathcal{K}$ is close to one the system is chaotic while $\mathcal{K}$ is close to zero, the system is nonchaotic. The zero-one for the proposed system can be described as follows:

$$\mathcal{K}_x = \mathbf{0.97706}, \mathcal{K}_y = \mathbf{0.99352}, \ \mathcal{K}_z = \mathbf{0.9408}, \mathcal{K}_w = \mathbf{0.99723}, \mathcal{K}_u = 0.99249$$

proved that system 2.1 is chaotic. Dissipative, Equilibrium, and Stability of Sine-Cosine Hyperchaotic 5-D System The system 2.1 exhibits different dynamical analysis as below:

If $-\alpha < \eta + \xi - \psi - \tau$, **then** $\nabla\nu \prec 0$, **the system 2.1 is dissipative.**

If $-\alpha = \eta + \xi - \psi - \tau$, **then** $\nabla\nu = 0$, **the system 2.1 is conservative.**

If $-\alpha > \eta + \xi - \psi - \tau$, **then** $\nabla\nu > 0$, **the system 2.1 is unbounded.**

The dissipative of a Sine-Cosine Hyper-chaotic 5-D System can be calculated as:
$\nabla\nu = \frac{\partial\dot{x}}{\partial x} + \frac{\partial\dot{y}}{\partial y} + \frac{\partial\dot{z}}{\partial z} + \frac{\partial\dot{w}}{\partial w} + \frac{\partial\dot{v}}{\partial v} = -\alpha - \eta - \xi - \psi - \tau$ =-19.4, therefore $\nabla\nu \prec 0$ proved that the system 2.1 is dissipative. The equilibrium points are calculated by setting R.H.S. equal to zero for system 2.1 as follows:

$$\left.\begin{array}{c} 0 = -\alpha\ x + \beta\ y - u\cos w \\ 0 = -\eta\ y\ + \sigma\ x - \mho\ \ x\ z + x\ \sin u \\ 0 = -\xi\ z\ + y\ x + \varrho\ \ w\ \ \sin x \\ 0 = -\psi\ u\ + \delta\ v\ z + y\ \sin z \\ 0 = -\tau w - y\ z - \ \eta\ x\ \sin y \end{array}\right\} \tag{2.2}$$

We concluded that from 2.2 that O_z one zero equilibrium point where O_z (0,0,0,0,0) We obtain the Jacobin matrix for system 2.1 by substitution the parameter and O_z We get:

$$\mathrm{j} = \begin{bmatrix} \alpha & \beta & 0 & u\mathrm{Sin}[w] & -\mathrm{Cos}[w] \\ \sigma + z\mho + \mathrm{Sin}[u] & -\eta & x\mho & 0 & x\mathrm{Cos}[u] \\ y + w\varrho\mathrm{Cos}[x] & x & -\xi & \varrho\mathrm{Sin}[x] & 0 \\ -\mathrm{Sin}[y] & -z - x\mathrm{Cos}[y] & -y & -\tau & 0 \\ 0 & -\mathrm{Sin}[z] & -w\delta - y\mathrm{Cos}[z] & -z\delta & -\psi \end{bmatrix}$$

$$j = \begin{bmatrix} -10.2 & 12 & 0 & 0 & -1 \\ 30 & -5.1 & 0 & 0 & 0 \\ 0 & 0 & -2 & 0 & 0 \\ 0 & 0 & 0 & -1 & 0 \\ 0 & 0 & 0 & 0 & -1.1 \end{bmatrix} \tag{2.3}$$

By using characteristic equation $|\lambda I - j| = 0$, from 2.3, we obtained $\lambda_1 = -26.7942$, $\lambda_2 = 11.4942$, $\lambda_3 = -2$, $\lambda_4 = -1.1$, $\lambda_5 = -1$, hence the system 2.1 at O_z is the saddle focus because it has one dimension unstable $\lambda_2 > 0$ and another dimension $\lambda_{1,3,4,5} < 0$ is a stable manifold, which proves that O_z unstable, since

$$677.556 + 1598.634\lambda + 1179.428\lambda^2 + 239.95\lambda^3 - 19.4\lambda^4 - \lambda^5 = 0 \tag{2.4}$$

By the calculated matrix Routh Hurwitz Criterion:

$$\begin{bmatrix} -1 & 234.95 & 1598.634 \\ -19.4 & 1179.428 & 677.556 \\ 179.1547 & 1563.7084 & 0 \\ 1348.7561 & 677.556 & 0 \\ 1473.7089 & 0 & 0 \\ 677.556 & 0 & 0 \end{bmatrix} \tag{2.5}$$

We get by using 2.5 the Sine-Cosine hyper-chaotic 5-D system 2.1 is **unstable**.

bounded Sine-Cosine Hyper-chaotic 5-D System

To prove the boundedness of the system 2.1 based on analytic and numerical methods. Assume all system parameters. $(\alpha, \beta, \ \eta, \sigma, \ \mho, \ \xi, \varrho, \psi, \delta, \tau) > 0$ and $x\,(0)\,,\ y\,(0)\,,\ z\,(0)\,,\ u\,(0)\,,\ w\,(0)$ are finite in R^5 to prove the state $(x(t), y(t), v(t), w(t), z(t))^T$ remain bounded for all t. pick $V = \frac{1}{2}\left(x^2 + y^2 + z^2 + w^2 + u^2\right) = \frac{1}{2}\|x\|^2$, therefore $V > 0$ for all non-zero states and $V = 0$ at the origin, along trajectory $\dot{V} = x\dot{x} + y\dot{y} + z\dot{z} + w\dot{w} + u\dot{u}$, by substitute

$$\dot{V} = \underbrace{-\alpha x^2 - \ \eta y^2 - \xi z^2 - \psi u^2 - \tau w^2}_{allways\ negative\ definite} + C \text{ , where}$$

$$C = \underbrace{(\beta + \sigma)\, xy + (1 - \mho)\, xyz + xysin\ u + \ \varrho wzsinx + \delta uwz - u\ sinz - wyz - \eta wxsiny + xucosw}_{bounded\ terms}$$

C bounded terms since trigonometric $|\sin(.)| \leq 1, |\cos(.)| \leq 1$ and cross terms are bounded using inequalities. $|uw| \leq \frac{1}{2}\left(u^2 + w^2\right)$, $|uwz| \leq \frac{1}{3}\left(u^2 + w^2 + z^2\right), \ldots$. therefore $\exists K > 0$ such that $C \leq K\sqrt{x^2 + y^2 + z^2 + w^2 + u^2}$ we concluded

$$\dot{V} \leq -\alpha_0(x^2 + y^2 + z^2 + w^2 + u^2) + K\sqrt{x^2 + y^2 + z^2 + w^2 + u^2}$$

Where $\alpha_0 = \min(\alpha, \eta, \xi, \psi, \ \tau)$, let $\mathbb{C} = \sqrt{x^2 + y^2 + z^2 + w^2 + u^2}$, so $\dot{V} \leq -\alpha_0\ \mathbb{C}^2 + K\mathbb{C}$. If $\mathbb{C} > \frac{K}{\alpha_0}$, then $\dot{V} \leq 0$. Therefore, the system is ultimately bounded. Fig.(4) shows the boundedness of the system 2.1, the blue attracted enclosed within is a semi-transparent dotted sphere.

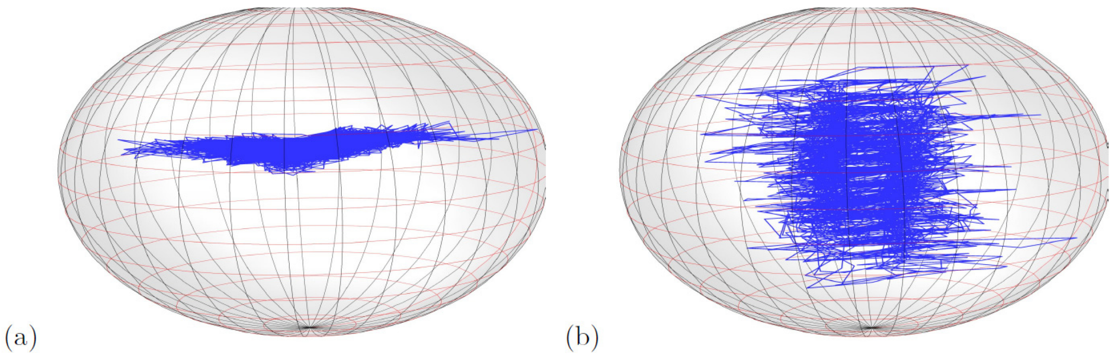

Figure 4: proves the boundness of a new sine-cosine hyperchaotic 5-D system.a) bounded with x-y-z plot b) bounded with w-y-x plot

3. Entropy and Dynamic Analysis

3.1. Entropy Analysis

Entropy measures are regarded as powerful tools that provide a comprehensive characterization of complicated dynamical systems across various fields [21]. They were originally formulated by Shannon (1948) [22] in the following form

$$H\,(y;\vartheta) = -E\,(ln\,(f(y;\vartheta))) \tag{3.1}$$

Where, $f\,(y;\vartheta)$ represents the density function of y. In the same context, Kolmogorov-Sinai entropy quantifies the rate of information production during the evolution of a chaotic system, thereby reflecting the amount of information lost or encoded over time. Pincus [23] proposed approximate entropy as a method for quantifying the complexity of time series data. It is worth noting that a fundamental relationship exists between Kolmogorov-Sinai entropy $KS_{entropy}$ and Lyapunov exponents $\lambda_i,\ i = 1, 2, .., n$ which was introduced by [24] in the following form:

$$KS_{entropy} = \sum_{\lambda_i > 0} \lambda_i \tag{3.2}$$

The entropy of system 2.1, evaluated for the parameters $\alpha, \beta,\ \eta, \sigma,\ \mho,\ \xi, \varrho, \psi$ and δ , is illustrated in Figure 5 with the initial condition (0.5, 2, 1.5, 6, 1). It is noteworthy that when the entropy values converge to zero, this implies that the system is either non-chaotic or that its chaotic behavior has nearly disappeared. Conversely, when the entropy values deviate from zero, this indicates the presence of chaotic dynamics. Evidently, the results presented in Figures (1–4) through chaotic dynamics analysis are in full agreement with the entropy behavior depicted in Fig.(5).

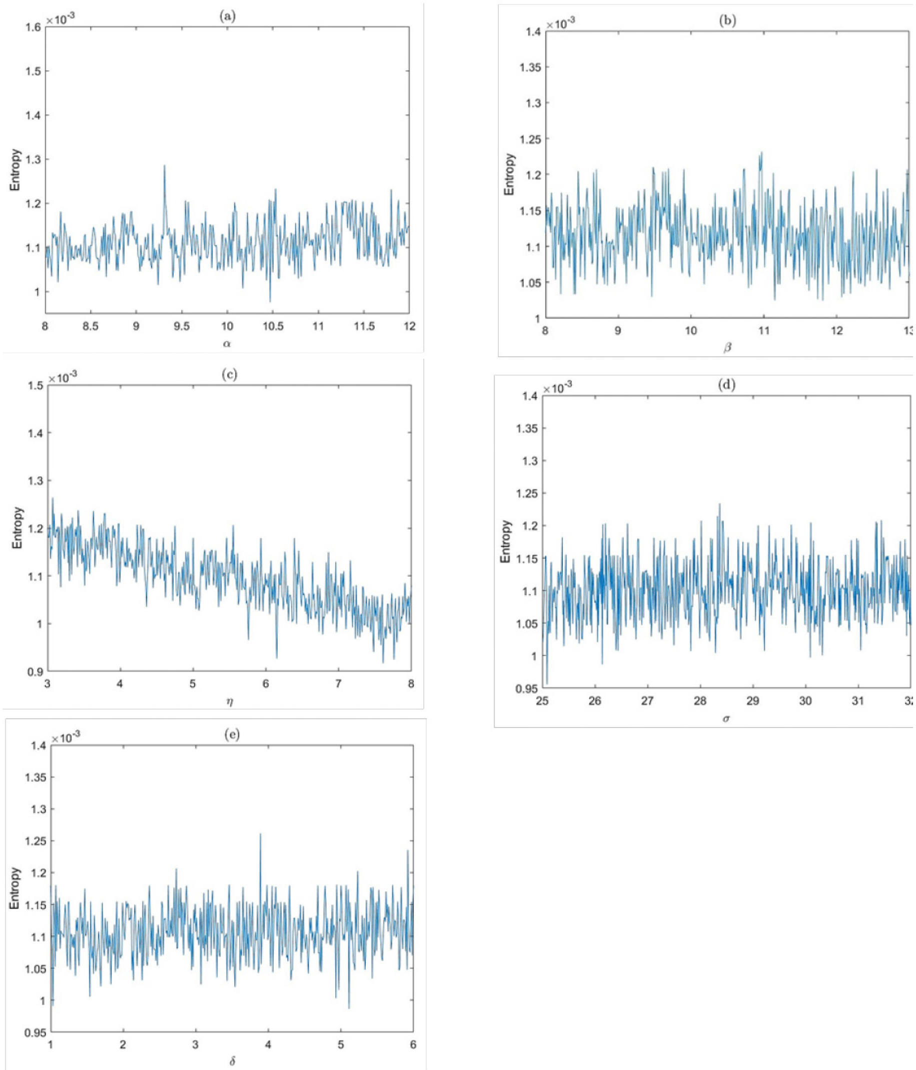

Figure 5: KS entropy vs. parameters of the system with initial state (0.5,2,1.5, 6, 1).

3.2. The Bifurcation Analysis

Analyze a bifurcation behavior to determine parameter ranges that induce a transition from stable state to chaotic behavior via periodic behavior. Hence studied case β as a control parameter in system 2.1. While β increases, the bifurcation diagram demonstrates that the system is undergoing some representative dynamical routes, such as stable fixed points, period-doubling flip route to chaos, which are summarized as follows:

β is shift, case $\beta \in [0, 1.734)$, and fixing residual parameter values has been stable and steady state with all $\mathfrak{L}_{\boldsymbol{i}}, \boldsymbol{i}=\mathbf{1},\ldots,\mathbf{5}$ are negative**,** from 2.3 yields a Jacobian matrix with 2*2 block corresponding to the variable x *and* y, $j_{2*2} = \begin{bmatrix} 10.2 & \beta \\ 30 & -5.1 \end{bmatrix}$ to find the critical value β_c set $|j_{2*2}| = 0$ as the result $\beta_c = 1.734$ at $\beta = \beta_c$ we obtained $\lambda_1(\beta_c) = 0$ and all other eigenvalues satisfy $Re\,(\lambda_{2,\ldots,5}) < 0$ first condition is satisfied since no pair of complex conjugate traverses the imaginary axis rules out a **Hopf bifurcation**. The eigenvalues $\lambda(\beta)$ satisfy characteristic equation $\lambda^2 + 15.3\ \lambda + (52.02 - 30\ \beta) = 0$, based on implicit derivatives and $\beta = \beta_c$ yields $\left.\frac{d\lambda}{d\beta}\right|_{\lambda=0} = \frac{30}{15.3} \neq 0$ transversality second condition satisfies. There exists **a non-oscillatory steady-state bifurcation** based on real bifurcation theorem at $\beta = \beta_c = 1.734$, also instability of O_z a zero equilibrium point arises from a real eigenvalue transitioning across zero. Case $\beta \in (1.734, 1.99]$ system 2.1 has a periodic attractor with one $\mathfrak{L}_1$ approximate to zero and $\mathfrak{L}_i, i=2,\ldots,5$ are negative,therefore there is a period-doubling flips window too, Case $\beta \in [2, 400]$ system 2.1 has the hyper-chaotic attractors with two positive $\mathfrak{L}_i, i=1, 2$. Fig. (6) display a numerical analysis at O_z Prove that system 2.1 has a non-oscillatory steady state bifurcation at $\beta_c = 1.734$ and route to chaos, with the bifurcation system 2.1 when transitioning from a stable state to chaotic behavior via periodic behavior as the parameter β increases with $\mathfrak{L}$ and $\wp_{KY}$.

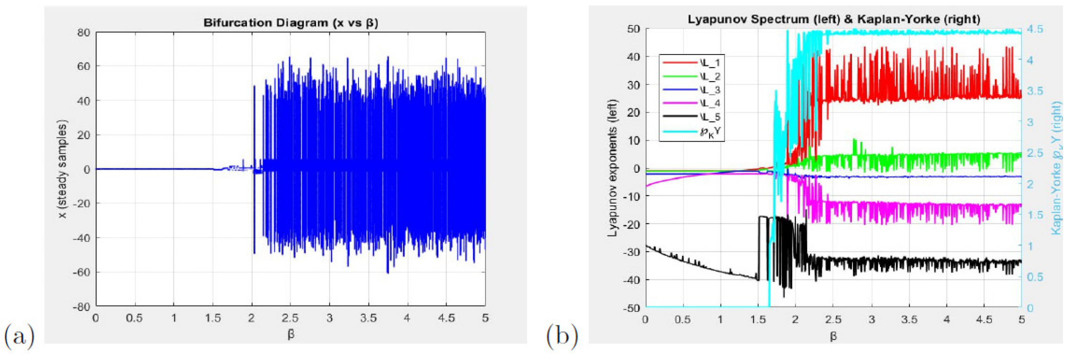

Figure 6: shows the bifurcation of a new sine-cosine hyper-chaotic 5-D system a) bifurcation diagram x state vs β and b)Lyapunov exponent vs β.

4. Proposed RGB Image Encryption Scheme

Applying 5-D sine-cosine hyperchaotic to RGB image encryption by using this system to generate the first technically generated SSMK by using the U, W sequence key, and second permute RGB image by using the W sequence key. Fig (8) Show the flowchart 5-D sine-cosine hyper-chaotic of the proposed RGB image encryption.

4.1. Algorithm to Generated $\boldsymbol{matrix}_{128\times128}$ (SSMK Generation)

The following step in this part can be summarized to produce a matrix whose some characteristics from the new Sine-Cosine hyper-chaotic system. This matrix is used to scramble color images as follows:

1. Set $(\alpha, \beta, \eta, \sigma, \mho, \xi, \varrho, \psi, \delta, \tau)$ as parameters and $x(0),\ y(0),\ z(0),\ v(0),\ w(0)$ as initial conditions for system 2.1

2. produced five sequences by applying the proposed system 2.1 , are x_i , y_i , z_i , w_i , and u_i where i = 1, 2,. . . , 65536.

3. Convert real numbers into a decimal number between 0 - 255 by using the following equation. And then the XOR operation between them
Result1 =XOR $(\mathbf{x_{i+1}=x_i\times10^{11}\ mod\ 256,\ y_{i+1}=y_i\times10^{11}\ mod\ 256})$

4. Convert result1 to $\boldsymbol{matrix}_{128\times128}$ have the following properties:
   (a) This matrix is symmetric.
   (b) Numbers between 0 to 255 are evenly distributed throughout each column and row without repeating.

Table 1. Showcase part of $\boldsymbol{matrix}_{128\times128}$, Fig. (7) display the process diagram to generate a matrix based on the SSMK generation algorithm, which is dependent on a sine-cosine 5-D hyper-chaotic system.

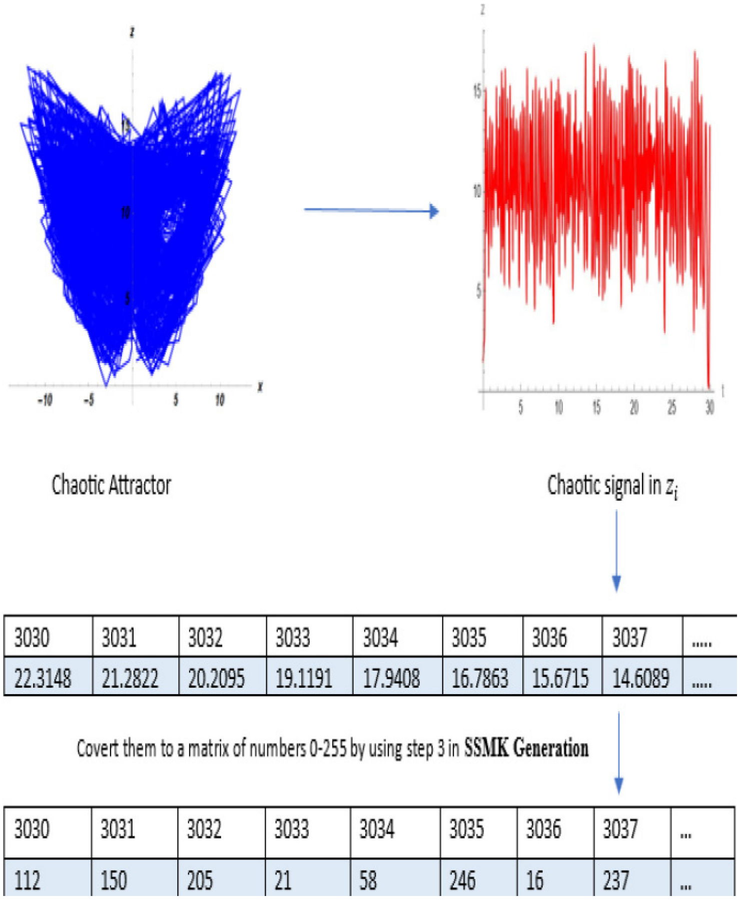

Figure 7: Displays the process diagram for the generated matrix based on the SSMK generation algorithm.

Table 1: Showcase partition of $matrix_{\ 128\times128}$ is SSMK $\boldsymbol{matrix}_{\ 16\times\mathbf{16}}$

0	183	27	15	225	230	222	14	26	134	174	216	42	145	170	91
183	99	66	186	94	33	147	102	81	50	192	98	110	7	253	152
27	66	170	218	224	63	241	231	162	199	33	14	164	60	44	226
15	186	218	31	8	214	93	152	146	137	44	181	243	77	58	202
225	94	224	8	35	184	125	147	85	38	114	191	217	135	23	44
230	33	63	214	184	158	252	151	60	81	195	10	50	128	233	177
222	147	241	93	125	252	225	248	24	177	245	218	189	71	18	46
14	102	231	152	147	151	248	3	212	82	194	174	205	61	158	130
26	81	162	146	85	60	24	212	90	120	56	91	197	165	133	94
134	50	199	137	38	81	177	82	120	49	234	229	139	247	30	64
174	192	33	44	114	195	245	194	56	234	187	62	204	233	208	17
216	98	14	181	191	10	218	174	91	229	62	53	160	157	168	131
42	110	164	243	217	50	189	205	197	139	204	160	51	117	78	213
145	7	60	77	135	128	71	61	165	247	233	157	117	47	15	28
170	253	44	58	23	233	18	158	133	30	208	168	78	15	223	65
91	152	226	202	44	177	46	130	94	64	17	131	213	28	65	84

4.2. Encryption Algorithm

Input: RGB image
Output: encryption of RGB image, secure keys including initial values and parameters of 5-D chaotic system
Begin:

1. Read the plain RGB image.
2. Resize it with size (256×256×3).
3. Split the RGB image into three Channels (Red, Green, and blue).
4. Apply a novel 5-D chaotic system to produce sequence keys including (X, Y, Z, W, U).
5. Apply sequence keys (U, W) to generate a secure symmetric matrix key (SSMK) with size (128 × 128).
6. For i:= 1 to 3 do:
   (a) Permutation operation: permute Ch_i by using (W) sequence key.
   (b) For k:= 1 to 256 step 128 do:
   (c) For j:= 1 to 256 step 128 do:
7. Encrypt C_{hi} [k : k+127 , j : j+127] := XOR operation between Ch_i [k : k+127, j : j+127] and SSMK.
8. End for$j$
9. End for$k$
10. End for$i$
11. Combination process: = Combine three channels to produce an encrypted RGB image.
12. Apply the Diffie-Hellman method to send secure keys that include parameters and initial values.
13. Send an encrypted RGB image to the receiver side.

End.

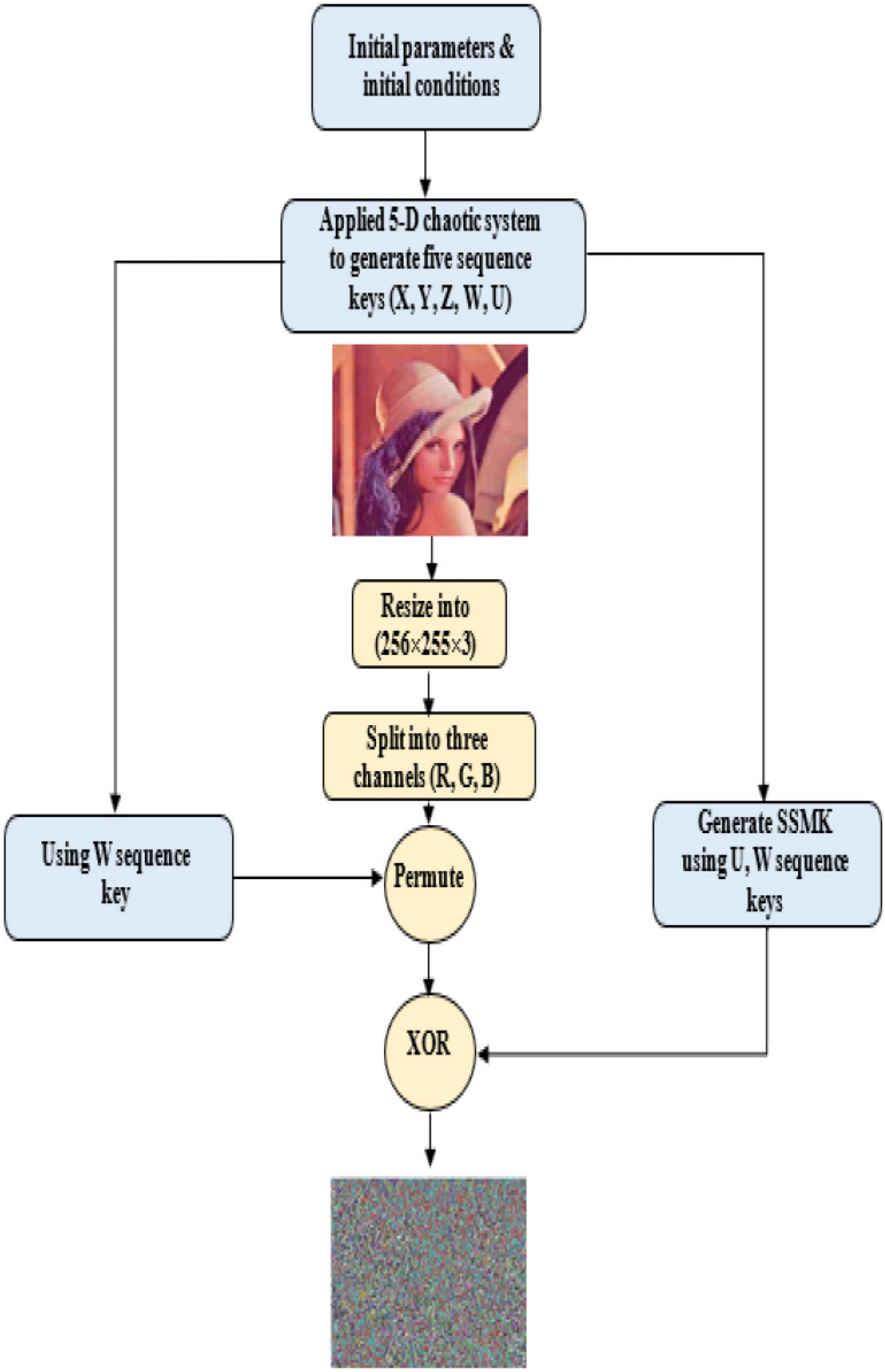

Figure 8: Show the 5-D sine-cosine hyperchaotic of the proposed RGB image encryption diagram.

Ultimately, transform the resultant sequence into an 8-bit binary format to yield random numbers and execute NIST tests to evaluate their randomness. Table 2 provides the NIST test findings for the sine-cosine 5-D hyperchaotic system, demonstrating that the sequences exhibit commendable pseudo-randomness.

Table 2: NIST SP800-22 tests

NIST-800-22 Tests	p-value					
	x	y	u	w	z	resentment
A. Entropy	0.6172	0.3496	0.3653	0.1957	0.5585	✓
Run	0.4074	0.4861	0.6748	0.9155	0.3417	✓
Rank	0.1626	0.1101	0.2113	0.6944	0.7916	✓
DFT	0.8839	0.1700	0.2932	0.5592	0.6196	✓
Non-Overlapping Template	0.0009	0.6474	0.0007	0.1957	0.3571	✓
Overlapping Template	0.2103	0.7600	0.7941	0.4527	0.3799	✓
Frequency	0.1792	0.5288	0.1038	0.0517	0.7326	✓
Block Frequency	0.7268	0.7309	0.2116	0.9799	0.9783	✓
Run	0.2825	0.9373	0.6960	0.74246	0.6648	✓
Serial -1 Serial -2	0.6387 0.7160	0.3290 0.2463	0.7128 0.7128	0.7801 0.5615	0.8410 0.7915	
Linear Complexity	0.9115	0.5913	0.6955	0.3754	0.9265	✓
Random Excursions	0.9103	0.8600	0.8941	0.4527	0.8799	✓
Random Excursion Variants	0.9792	0.9288	0.9038	0.9517	0.7326	✓
Universal Statistical	0.7268	0.8309	0.8113	0.9799	0.2783	✓

5. Analysis of Security Factors and Computational Results

In this section, we explore an examination of the RGB image encryption scheme to verify its effectiveness and security for the suggested method. A set of statistics is conducted on the images that have undergone the encryption process. We provided analysis and results on these findings in this research. We examined the performance of the algorithm in contrast to competing algorithms by comparing our results with those from different researchers, to demonstrate that the designed algorithm possesses a high level of resilience against statistical attacks. Several analyses have been conducted, including assessments of histogram distribution, keyspaces, key SDIC [25] , MSE, speed performance, NPCR, UACR, time run, correlation analysis, and information entropy, applied to the proposed scheme with different images. An Intel(R) 6 Core^{TM} i7- 10850H CPU, 2.70GHz, RAM (12GB) with MATLAB (R2021b) is required to evaluate the suggested encryption method. The effectiveness of the suggested technique was evaluated on various standard RGB images, such as (**Lena, Baboon, Airplane, splash, and Tree**) from SIPI images. Table 4. Illustrates in seconds the encryption time, which is exceptionally brief, making it one of the top-performing algorithms currently available for RGB images.

5.1. Keyspaces Analysis

The size of the keyspace plays a pivotal role in the technique of encryptionn[16,26] . If the keyspace size exceeds 2^{100} then the technique of encryption is resistant to statistical attacks. Assuming the precision of the I.C. values is 10^{16}, Fourteen security keys are $((\alpha, \beta,\ \eta, \sigma,\ \mho,\ \xi, \varrho, \psi, \delta, \tau)$ as parameters and $x(0),\ y(0),\ z(0),\ v(0),\ w(0)$ as initial conditions) included in the suggested method. Adding an average of 30 variables (because the system is used 2 times) to the entire encryption. We calculated the size of keyspaces is $10^{480} \approx 2^{1584}$ which proved that the keyspace was very large enough to be resistant to statistical attacks. Table 3 compares keyspaces for this scheme based on a new sine-cosine 5-D hyper-chaotic system with another scheme.

Table 3: compares keyspaces between our algorithm and another scheme

Ours, Refs	[27]	[16]	[28]	[29]	[30]	[31]	[32]	[33]	Our
Keyspaces	2^{279}	2^{512}	2^{554}	2^{626}	2^{170}	2^{233}	2^{711}	2^{170}	$\mathbf{2^{1584}}$

5.2. Key sensitivity analysis

The secret key used in the encryption process must be sensitive to the cipher key. The secret key 5-D sine-cosine hyper-chaotic of the proposed RGB image encryption are $(\alpha, \beta,\ \eta, \sigma,\ \mho,\ \xi, \varrho, \psi, \delta\ (0)\,,\ y\,(0)\,,\ z\,(0)\,,\ v\,(0)\,,\ w\,(0))$, just tiny changes in one value of keys and maintaining all the other parameters without change during the implemented image encryption. This sensitivity should result in a noticeable alteration in the encrypted image when recovering the plain image. The suggested algorithm has stronger key sensitivity and the ability to resist exhaustive attacks. Fig 9. shows the house image where a) the plain image with $\alpha = 10.2,\ \beta = 12,\ \eta = 5.1,\ \sigma = 30,\ \mho = 2.5,\ \xi = 6,\ \rho = 3,\ \psi = 1.1,\ \boldsymbol{\delta = 4}$, and $x\,(0) = 0.5,\ y\,(0) = 2,\ z\,(0) = 1.5,\ v\,(0) = 6,\ w\,(0) = 1$, b) encrypted house image, c) decrypted image without changing key security, d) decrypted image with changing key security $\boldsymbol{\delta = 4 \times 10^{-14}}$ Other keys unchanged.

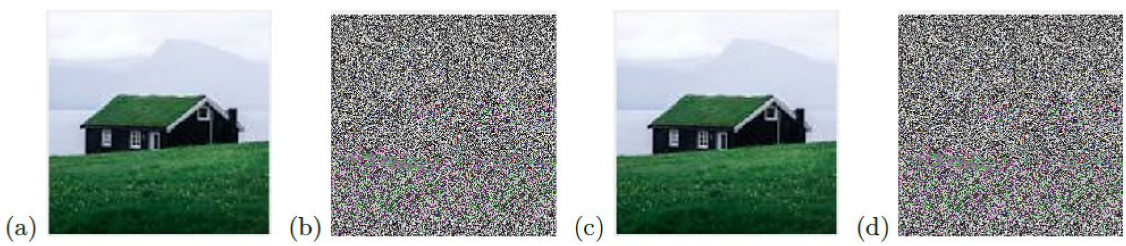

Figure 9: shows the key sensitivity of the house image.

5.3. Information Entropy Test

Entropy is a critical factor for measuring randomness in information[16], [26]**.** To establish the robust security of the suggested scheme and its resilience against various types of attacks, we can draw upon the statistical evidence provided by the range (7.9990 - 7.9998). This range signifies that the plain image exhibits a lower level of randomness compared to the ciphered image. The entropy values for the suggested method taken for various images are all close to 8. Table 4 showcases the calculated entropy for this scheme based on a new sine-cosine 5-D hyperchaotic system with different RGB images.

5.4. Correlation Coefficient Test

In general, the connection **r** between neighboring pixels in the plain images for three dimensions: vertical V, diagonal D, and horizontal H described as strong with most between ± 1. This correlation must be reduced close to zero for an encryption method to be effective. The suggested algorithm was computed and analyzed to assess the spatial associations among neighboring pixels in both the plain and scrambled images. Every result in the scrambled image shows that the approach we've suggested can eliminate the association between neighboring pixels. Table 4 shows the correlation (r) for different images and **Table 6.** compares r for this scheme based on a new sine-cosine 5-D hyper-chaotic system with another scheme. **Fig. (10)** showcases the calculated correlation pixel r for a scramble along three directions, H, D, and V, respectively.

5.5. NPCR, UACI tests

UACI quantifies changes in mean intensity that are used to test for sensitivity, besides NPCR, which evaluates the number of distinct pixels impacted. The objective of the attacker is to descramble the scrambled images without utilizing the key security, primarily by identifying the correlation between the plain and scrambled images. Consequently, even slight alterations can exert a substantial influence on the scrambled image, thereby markedly increasing the challenge for attackers attempting to breach the encryption. Successful image encryption algorithms must be resilient against this form of attack. In Table 4, you can observe the NPCR and UACI values calculated for different RGB images. All values NPCR and UACI are close to ideal values. These results from our experiment underscore the high level of resistance exhibited by the suggested algorithm against various attacks.

5.6. MSE and PSNR Tests

We apply MSE and PSNR as follows.

$$\textbf{squaredErrorImage} = (\textbf{double(image)} - \textbf{double(scrambled)})^{2}$$

$$\textbf{MSE} = \textbf{sum(squaredErrorImage(:))} \;/\; \textbf{(rows . columns)}$$

$$\textbf{PSNR} = \textbf{10} * log_{10} \left(\frac{\textbf{255}^2}{MSE} \right)$$

In Table 4. We can observe the MSE and PSNR values calculated for different RGB images. All values of PSNR are lower ideal values furthermore, superior MSE values are shown.

5.7. Histogram Test

Histogram analysis gives an idea to statistical analysis attackers, but in this suggested method, by the use of histograms, the attackers cannot find any clue about the plain image. To safeguard the information contained within an original image from potential attackers, the statistical features of the plain and scrambled image must exhibit significant disparities. Fig.(11) displays a simulation from the results of the suggested algorithm to show different histograms between the plain and scrambled image.

Table 4: Calculated and analyzed for different scrambled RGB images.

Image	r for three-direction			Entropy	MSE	PSNR	NPCR%	UACI%	Time scram-bled
	D.	**H.**	**V.**						
Airplane	-0.0014	0.0008	0.0012	7.9998	1040	7.9941	99.6032	33.4611	0.0033
Lena	−0.0006	0.0004	0.0009	7.9992	9994	8.6576	99.6098	33.4599	0.0035
Baboon	-0.001	0.00008	0.0019	7.9991	8227	9.0123	99.6180	33.3692	0.0036
peppers	-0.0007	0.00054	0.0010	7.9992	1006	8.1365	99.5651	33.1921	0.0035
Splash	-0.0012	0.00115	0.0015	7.9998	1126	7.6475	99.6231	33.0694	0.0037
Tree	0.0112	0.00073	0.0012	7.9998	8927	8.1670	99.6032	33.0706	0.0035

6. Result and Discussion

We explore the comparison and the advantage of a new Sine-Cosine two-wing 5-D hyperchaotic system on the results. Table 5. Comparing the analysis sine - cosine 5-D hyper-chaotic system 2.1 , which consisted of nine non-linear terms out of sixteen terms, with the different 5-D systems in the previous paper. The proposed system 2.1 provides benefits. Which involve higher $\mathfrak{L}$= 15.0210, and greater $\wp_{KY}$=4.8675, highly SDIC, proved that multistability, two wing attractors, and two positives $\mathfrak{L}$.We prove how the transition from stable to chaotic state via a bifurcation diagram, also we prove the proposed system is bounded; furthermore, we compare and analyze a new Sine-Cosine two-wing 5-D hyper-chaotic system in RGB image encryption. Table 6. Comparing the analysis of RGB image encryption with the existing algorithms in the previous paper. The proposed methods for encryption provide benefits. This involves speed time scrambling 0.0033, representing a shorter time than other papers, proving that encryption is lightweight.2^{1488} This proved that the keyspace was very large enough to be resistant to statistical attacks, the entropy values 7.9998 are all close to 8 for the suggested method, and the r values 0.0009 refer to the mean correlation value between neighboring pixels along the V., H., and D. directions within the Lena image. represent lower than other papers.

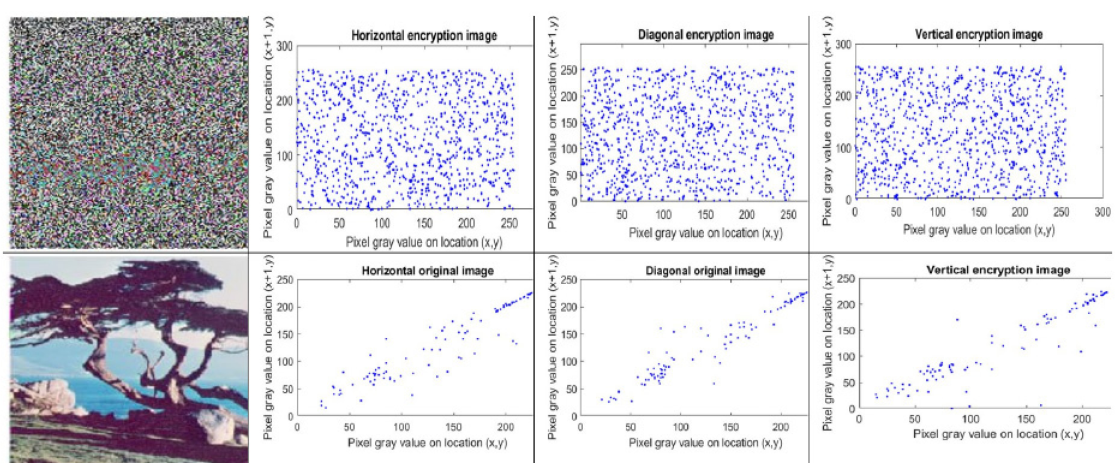

Figure 10: showcases the Comparison correlation pixel for a scramble along three directions, H, D, and V, respectively.

Table 5: Comparing the analysis sine -cosine 5-D hyper-chaotic with the different 5-D in the previous paper.

Year	**Refs.**	**Maximum $\mathfrak{L}$**	$\wp_{KY}$	**Number of positive L_e**	**Number of terms Non-linear**	**Total**
2019	[34]	0.1	-	0ne	3	8
2022	[35]	8.5892	3.2776	two	4	13
2020	[36]	-	-	-	5	12
2020	[13]	> 0	-	two	6	11
2007	[37]	0.01962	-	one	11	16
2020	[38]	0.72182	2.6673	two	7	15
2021	[39]	2.512	3.1325	two	3	14
2018	[40]	0.3714	4.0292	two	3	12
[h] 2018	[41]	-	-	three	6	14
2020	[42]	> 0		one	3	11
2021	[43]	-	-	-	3	13
2022	[44]	12.659	4.189	three	3	13
2013	[6]	0.555555	4.0849	three	3	12
2014	[45]	0.4195	4.0159	three	3	12
2017	[7]	9.979	3.6243	three	3	11
2020	[38]	0.72182	2.6673	two	3	15
2022	[46]	1.5839	4.0	two	7	18
2023	[47]	0.3049	4.3801	three	4	10
2024	[[48]]	14.291	4.8666	three	4	13
Our		**15.0210**	**4.8675**	**two**	**9**	**16**

7. Conclusion Summarizing the Key Findings and Insights

This work introduces the new Sine-Cosine two-wing 5-D system and analyzes system 2.1 which proved hyper-chaotic dynamical behavior has a high complexity attractor by different analyses, symmetric, SDIC, Kaplan-Yorke dimension, zero-one test, multistability, Lyapunov exponent, dissipative, equilibrium pt., stability proposed systems, and Routh stability, found that system 2.1 has 2+ve $\mathfrak{L}$, maximum $\mathfrak{L}$, and superior Kaplan-Yorke Dimension compression with all system 5-D different lecturer previous. We are applying a 5-D sine-cosine hyperchaotic to produce a matrix (SSMK Generation), which has special properties that enable us to benefit from it in RGB Image encryption. Furthermore, we used system 2.1to create an RGB image scrambler scheme to give a better level of security. It has proven the efficiency and speed performance of image encryption. Comparing the analysis of RGB image encryption with the existing algorithms in the previous paper. Found that shorter than other papers proving that encryption is fast, the keyspace was very large enough to be resistant to statistical attacks, the entropy values were all close to 8, and the r mean values were. Represent lower than other papers using different images. In future work, the system can be used in other fields such as circuit design, feedback control, medical image, multimedia encryption, etc

Table 6: Comparing the analysis of RGB image encryption with the existing algorithms in the previous paper.

methods	r for three-direction			Entropy	MSE	PSNR	NPCR%	UACI%	Time scrambled
	D.	**H.**	**V.**						
Ours	-0.0006	0.0004	0.0009		9994	7.6475	99.6231	3.4611	0.0033
[28]	0.0031	0.0015	0.0030	7.9989	8923	8.6256	99.6246	30.5681	3.0608
[49]	0.0006	0.0009	0.0021	7.9994	869.8890	9.7971	99.6085	33.4624	1.0896
[33]	0.0034	0.0002	0.0028	7.9994	-	8.6091	99.6101	33.4641	0.9047
[50]	0.0004	0.0004	0.0004	7.9956	7119.13	8.1060	99.5890	30.1260	12.75
[51]	-	-	-	7.9998	-	-	99.6473	33.5516	0.085
[31]	0.0043	0.0035	0.0020	7.9967	-	-	99.8480	33.2689	-
[52]	0.0119	0.0096	0.0109	7.9998	8923	8.6256	99.6062	33.4623	3.0608
[53]	-	-	-	7.9988	-	-	99.6112	33.4254	2.12

Acknowledgments

The authors would like to thank the editor and the anonymous reviewers for their valuable comments and suggestions, which greatly improved the quality of this paper.

References

1. K. A. Abro, and A. Atangana,, *Strange attractors and optimal analysis of chaotic systems based on fractal verses fractional differential operators*, Int. J. Model. Simul, 42, 5, 716–724,(2022).
2. S. H. Abid and U. J. Quaez , *Capacity of control for stochastic dynamical systems perturbed by mixed fractional brownian motion with delay in control*, Int. J. Innov. Comput. Inf. Control,15, 5, (2019).
3. U. J. Quaez ,*Dynamics And Entropy Analysis Of A Novel Fractional Chaotic System For Color Medical Image Encryption* ,Int. J. Innov. Comput. Inf. Control, 21, 4, (2025).
4. S. B. Sadkhan ,*Bifurcation of Novel Seven-Dimension Hyper Chaotic System*. in. Journal of Physics: Conference Series ,IOP Publishing, (2021).
5. K. Benkouider ,*A new 10-D hyperchaotic system with coexisting attractors and high fractal dimension: Its dynamical analysis, synchronization and circuit design* ,PLoS One, 17, 4, , (2022).
6. Q. Yang and C. Chen ,*A 5D hyperchaotic system with three positive Lyapunov exponents coined*, Int. J. Bifurc. Chaos, 23, 6, (2013).
7. Y. Li ,C. Wang , and H. Chen ,*A hyper-chaos-based image encryption algorithm using pixel-level permutation and bit-level permutation* , Opt. Lasers Eng, 90,238–246, (2017).
8. S. Sun,*A novel hyperchaotic image encryption scheme based on DNA encoding, pixel-level scrambling and bit-level scrambling*. IEEE Photonics J., 10, 2, 1–14, (2018).
9. S. Vaidyanathan, L. G. Dolvis, K. Jacques, C. H. Lien, and A. Sambas,*A new five-dimensional four-wing hyperchaotic system with hidden attractor, its electronic circuit realisation and synchronisation via integral sliding mode control* . Int. J. Model. Identif. Control, 32, 1, 30–45, (2019).
10. D. Fang and S. Sun,*A new secure image encryption algorithm based on a 5D hyperchaotic map*. PLoS One, 15, 11, e0242110, (2020).

11. T. Wang, L. Song, M. Wang, and Z. Zhuang,*A novel image encryption algorithm based on parameter-control scroll chaotic attractors*. IEEE Access, 8, 36281–36292, (2020).

12. C. Xu, X. Wu, Y. He, and Y. Mo, *5d hyper-chaotic system with multiple types of equilibrium points*. J. Shanghai Jiaotong Univ., 25, 5, 639–649, (2020).

13. F. Yu et al.,*Chaos-based application of a novel multistable 5D memristive hyperchaotic system with coexisting multiple attractors*. Complexity, (2020).

14. M. Kaur and D. Singh,*Multiobjective evolutionary optimization techniques based hyperchaotic map and their applications in image encryption* . Multidimens. Syst. Signal Process, 32, 1, 281–301, (2021).

15. S. J. Sheela, A. Sanjay, K. V Suresh, D. Tandur, and G. Shubha, *Image encryption based on 5D hyperchaotic system using hybrid random matrix transform*. Multidimens. Syst. Signal Process, 33, 2, 579–595, (2022).

16. H. A. Ismael and and etal,*Image scrambler based on novel 4-D hyperchaotic system and magic square with fast Walsh–Hadamard transform* . Bull. Electr. Eng. Informatics, 11, 6, 3530–3538, (2022).

17. M. E. Manaa, S. S. A. Al-Murieb, and F. J. Abd Al-Razaq,*Analysis and description S-box generation for the AES algorithm-a new 3D hyperchaotic system* . Bull. Electr. Eng. Informatics, 12, 3, 1639–1647, (2023).

18. M. A. A.-K. AL-Yaseen,*Shadowing, limit shadowing and two-sided limit shadowing* . J. Interdiscip. Math., 24, 5, 1133–1135, (2021).

19. S. A. Mehdi and and etal,*Design and Analytic of A Novel SevenDimension Hyper Chaotic Systems* . 1st. Information Technology To Enhance e-learning and Other Application (IT-ELA, IEEE, (2020).

20. M. A. A.-K. AL-Yaseen,*Some chaotic properties of 2-D rational discrete map,* . J. Interdiscip. Math., 24, 5, 1127–1131, (2021).

21. S. H. Abid and U. J. Quaez,*Rényi entropy for mixture model of ultivariate skew normal-cauchy distributions* . J. Theor. Appl. Inf. Technol. 97, 13, (2019).

22. C. E. Shannon, *A mathematical theory of communication*. Bell Syst. Tech. J., 27, 3, 379–423, (1948).

23. S. M. Pincus,*Approximate entropy as a measure of system complexity* . Proc. Natl. Acad. Sci., 88, 6, 2297–2301, (1991).

24. J. B. Pesin, *Ljapunov characteristic exponents and ergodic properties of smooth dynamical systems with an invariant measure*. Hamiltonian Dynamical Systems, CRC Press, (2020).

25. H. K. Zghair,*Analysis of novel seven-dimension hyper chaotic by using SDIC and waveform* . 3rd International Conference on Engineering Technology and its Applications (IICETA), IEEE, 95–99,(2020).

26. S. B. Sadkhan,*Speech scrambler based on discrete cosine transform and novel seven-dimension hyper chaotic system* . Journal of Physics: Conference Series, IOP Publishing, , 12048, (2021).

27. S. Zhou, Y. Qiu, G. Qi, and Y. Zhang,*A new conservative chaotic system and its application in image encryption* . Chaos, Solitons , Fractals. 175, 113909, (2023).

28. M. T. Elkandoz and W. Alexan, *Image encryption based on a combination of multiple chaotic maps*. Multimed. Tools Appl., 81, 18, 25497–25518, (2022).

29. B. Stoyanov and K. Kordov, *Image encryption using Chebyshev map and rotation equation*. Entropy, 17, 4, 2117–2139, (2015).

30. L. Huang, W. Li, X. Xiong, R. Yu, Q. Wang, and S. Cai, *Designing a double-way spread permutation framework utilizing chaos and S-box for symmetric image encryption*. Opt. Commun., 517, 128365, (2022).

31. X. Wei, L. Guo, Q. Zhang, J. Zhang, and S. Lian, *A novel color image encryption algorithm based on DNA sequence operation and hyper-chaotic system*. J. Syst. Softw., 85, 2, 290–299, (2012).

32. R. Hamza and F. Titouna, *A novel sensitive image encryption algorithm based on the Zaslavsky chaotic map*. Inf. Secur. J. A Glob. Perspect., 25, 4–6, 162–179, (2016).

33. L. Huang, S. Cai, X. Xiong, and M. Xiao,*On symmetric color image encryption system with permutation-diffusion simultaneous operation* . Opt. Lasers Eng.,115, 7–20, (2019).

34. A. Ahmadi, K. Rajagopal, V.-T. Pham, O. Boubaker, and S. Jafari,*A new five dimensional multistable chaotic system with hidden attractors* . Recent advances in chaotic systems and synchronization, Elsevier, 77–87, (2019).

35. Y. Tong, Z. Cao, H. Yang, C. Li, and W. Yu, *Design of a five-dimensional fractional-order chaotic system and its sliding mode control*. Indian J. Phys., 96, 3, 855–867, (2022).

36. T. Wang, L. Song, M. Wang, S. Chen, and Z. Zhuang, *A novel Five-Dimensional Three-Leaf Chaotic Attractor and its application in image encryption*. Entropy, 22, 2, 243, (2020).

37. X. Jiang, D. Yuan, and Y. Xiao,*Chaotic dynamics of a five-dimensional nonlinear network* . Int. J. Mod. Phys. C, 18, 03, 335–342, (2007).

38. S. Mehdi, and Kadhim A., *Design and Analysis of a Novel Five-Dimensional Hyper-Chaotic System* , dynamics, 15, 16, (2020).

39. J. Mostafaee , S. Mobayen , Vaseghi B., and M. Vahedi ,*Finite–time synchronization of a new five–dimensional hyper–chaotic system via terminal sliding mode control* , Sci. Iran., (2021).

40. Y. Sui, Y. He, W. Yu, and Y. Li,*Design and circuit implementation of a five-dimensional hyperchaotic system with linear parameter* ,Int. J. Circuit Theory Appl, 46, 8, 1503–1515, (2018).

41. C. C. Felicio and P. C. Rech, *On the dynamics of five-and six-dimensional Lorenz models*, J. Phys. Commun., 2, 2, (2018).

42. Y. Huang,*A five-dimensional grid multi-wing butterfly chaotic system and its circuit simulation* ,Journal of Physics: Conference Series, IOP Publishing, (2020).

43. T. D. Nguyen, T. T. Dieu Phan, and R. Jašek, *Parameter estimation in five dimensions chaotic synchronization systems by self-organizing migrating algorithm*, WSEAS Trans. Syst., (2012).

44. K. Benkouider, *A New 5-D multistable hyperchaotic system with three positive lyapunov exponents: bifurcation analysis, circuit design, FPGA realization and image encryption*, IEEE Access, 10, 90111–90132, (2022).

45. S. Vaidyanathan, C. Volos, and V.-T. Pham,*Hyperchaos, adaptive control and synchronization of a novel 5-D hyperchaotic system with three positive Lyapunov exponents and its SPICE implementation* , Arch. Control Sci., 24, 4, (2014).

46. S. S. Ahmed and S. A. Mehdi, *Image Encryption Algorithm based on A Novel 5D Chaotic System*, 8th International Conference on Contemporary Information Technology and Mathematics (ICCITM), IEEE,249–255, (2022).

47. S. F. Al-Azzawi and A. M. Hasan, *New 5D hyperchaotic system derived from the Sprott C system: Properties and anti synchronization*, J. Intell Syst. Control, 2, 2, 110–122, (2023).

48. H. K. Zghair,*Design and analysis of a novel self-excited 5-D hyperchaotic system with maximum (n-2) positive lyapunov exponents* , J. Discret. Math. Sci. Cryptogr., 27, 5, 33–39, (2024).

49. L. Huang, S. Cai, M. Xiao, and X. Xiong,*A simple chaotic map-based image encryption system using both plaintext related permutation and diffusion* , Entropy, 20, 7,(2018).

50. T. ul Haq and T. Shah, *12× 12 S-box design and its application to RGB image encryption*. Optik (Stuttg), 217, 164922, (2020).

51. K. A. K. Patro and B. Acharya,*An efficient colour image encryption scheme based on 1-D chaotic maps*,J. Inf. Secur. Appl., 46, 23–41, (2019).

52. H. Qiu, X. Zhang, H. Yue, and J. Liu,*A Novel Eighth-Order Hyperchaotic System and Its Application in Image Encryption* , Mathematics, 11, 19, (2023).

53. Y. Wu, L. Zhang, S. Berretti, and S. Wan, *Medical image encryption by content-aware dna computing for secure healthcare* ,IEEE Trans. Ind. Informatics, 19, 2, 2089–2098,(2022).

Hayder Kadhim Zghair,
Department of Software,
Information Technology College, University of Babylon,
Iraq.
E-mail address: hyderkkk@uobabylon.edu.iq

and

Adil Khudhair Bagheedh,
Department of Mathematics, Education College,
Mustansiriyah University,
Iraq.
E-mail address: aaddeel83@uomustansiriyah.edu.iq

and

Uday Jabbar Quaez,
Department of Mathematics, Education College,
Mustansiriyah University,
Iraq.
E-mail address: dr.uday@uomustansiriyah.edu.iq